Mechanical Properties and Phase-Transition of Laser-Deposited Sol-Gel Titania Coatings

Y. Adraider
Tajoura Research Center
yadraider@yahoo.com

Abstract **- Titanium oxide coatings were fabricated via a combaine laser/sol-gel technique. The deposition of sol-gel titania coatings on AISI316 substrates is conducted using fibre laser irradiation (λ=1064 nm) in continuous wave mode under wet condition with different laser specific energies. ATR-FTIR, XRD, SEM and EDS were used to investigate the phase composition, crystalline structure, surface morphology of the laser-deposited titania coatings, whilst the mechanical properties were measured using nano-indentation. The results illustrate that the laser irradiation led to the deposition of titanium oxide coatings in both crystalline phases, anatase and rutile at various processing conditions. The optimal theoretical ratio of 1:2 in TiO2 is obtained for the deposited titania coatings under the influence of laser energy. Nano-indentation measurements confirm that the mechanical properties of laser-deposited titania coatings are significantly improved.**

Keyword-Sol-gel Titania coatings; Fiber Laser; titanium Oxide; Mechanical properties

I. INTRODUTION

Ceramics provide a beneficial solutions for various engineering applications to improve the properties and the micro-structure of metals in terms of the oxidation and corrosion resistance, mechanical performance and increasing the lifetime of the products. Titanium oxide as one of the ceramic materials has been paid much attention in the last decades according to its unique properties such as excellent corrosion resistance [1], high mechanical stability, self-cleaning surfaces , low cost and thermostability [2,3]. Titanium oxide can be found in three different crystal forms including rutile, anatase and brookite. The rutile and anatase can be classified as stable forms, whilst brookite is known as unstable form, the rutile-TiO_2 is the most usable and preferable phase among of them [4-6]. The crystallisation of titanium oxide coatings depends on the heating temperature either as powder or coated on the substrate. Titanium oxide is an attractive and ideal material to utilise for a wide range of applications such as gas sensors, medical implants, aerospace, photovoltaic devices, marine and automotive [7-10]. Sol-gel method has employed to prepare ceramic thin films because of its low processing temperature, low cost, high purity coatings and simple technique. Variety of variables can affect the sol-gel process in terms of reaction conditions, for instance solvent, pH, composition, temperature, molar ratios and concentration.

This research paper aims to employ the fibre laser to deposit the sol-gel titania coatings on AISI316 substrates under wet condition. Different analysis techniques were used to characterise the properties, phase structure and composition of the laser-deposited titania coatings.

II. II. EXPERIMENTAL

A. Sample Preparation

Titania sol was prepared by sol-gel technique. Titanium butoxide (99%) (precursor) was dissolved in isopropanol (solvent), then added into a mixture of distilled water and nitric acid (stabiliser), under vigorous stirring. The reaction system was kept stirring at 65°C for several hours until the system became completely transparent, indicating that a colloidal titania dispersion is formed. All chemicals were purchased from Sigma-Aldrich and used as-received.

Stainless Steel AISI316 substrates were cut into small rectangular pieces approximately 20x12x2 mm^3, followed by polishing the surfaces with grit SiC sand papers through different stages, ended at 6μm diamond paste. The polished surfaces then washed with distilled water and dried in the air. The chemical composition of AISI316 is listed in Table I.

Table I. Chemical composition of the SS316 used.

C %	Mn %	Si %	P %	S %	Cr %	Mo %	Ni	N %	Fe %
0.08	2.0	0.8	0.05	0.03	16.0-18.0	2.0-3.0	10.0-14.0	0.1	balance

The deposition of titanium oxide coatings into AISI316 substrates was conducted using fibre laser (SPI G3.0 Fiber Laser Module, SIP Laser UK, Ltd), with wavelength of λ=1064 nm at continuous wave mode (CW). A circular laser beam with spot diameter of 23 μm was focused during the scanning process, and the scanning area was designed as rectangular shape a 10x6 mm^2, with distance of 20 μm between the scanning lines to cover the whole scanning area. Different laser energies were used to deposit the titanium oxide coatings on (AISI316) substrates. The laser energies employed to induce the deposition of sol-gel titania coatings are 8.7 J/mm^2, 10.9 J/mm^2 and 21.7 J/mm^2. A rectangular plastic mould was carefully fixed

on the substrate surface in order to prevent the leakage of titania sol between the mould and the substrate surface, as well as controlling the coating thickness. Titania sol was charged into the mould, and then scanned immediately. The thickness of the titania sol during laser scanning was found approximately 1mm. The experimental procedure is shown in Fig. 1.

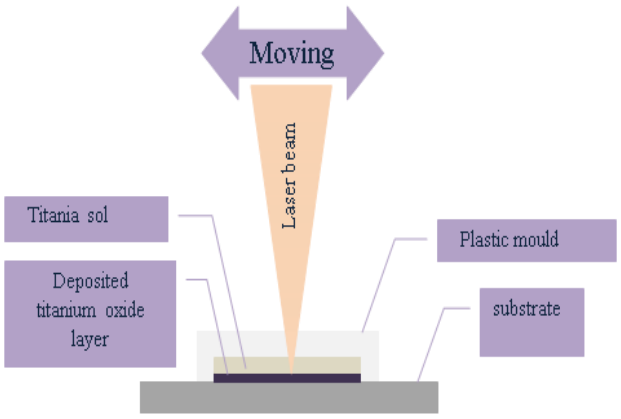

Figure 1. Experimental set-up

B. Characterisation

Attenuated total reflectance Fourier transform infrared spectroscopy (ATR-FTIR) was used on a Thermo Necolet 5700 FTIR spectroscope to analyse the laser-deposited titania coatings. All spectra were taken in a uniform range of wavenumber between 400 and 4000 cm^{-1} at 4 cm^{-1} resolution, with averaging over 32 scans.

X-ray diffraction (XRD, Siemens D500 X-ray diffractometer) with CuKα radiation at 20 mA and 40 kV, was conducted to determine the phase composition of laser-deposited titania coatings. The 2θ range for each diffractionattern was acquired from 20˚ to 70˚ in step size of 0.02˚ and step time 1 s.

SEM electron microscopy (Hitachi 3400 N, Japan) was employed to study the surface morphology and microstructure of the laser-deposited titania coatings. Elemental composition of the laser-deposited titania coatings was carried out using the energy dispersive spectroscopy (EDS – Oxford Instrument, UK).

Nan indentation technique (Nano Test™, Mateial Ltd, UK) was used to determine the hardness (H) and Young's modulus (E) of the laser-deposited titanium oxide coatings.

III. III. RESULTS AND DISCUSSION

A. ATR-FTIR Analysis

The change of chemical composition of sol-gel titanium oxide coatings under the influence of laser energies was conducted through ATR-FTIR spectroscopy. Fig. 2, displays the ATR-FTIR spectra of the deposited titania coatings at various laser energies. As can be clearly seen, the as-prepared sample (as reference) illustrates absorption peaks: the peak at 730 cm^{-1} refers to Ti-O bond [11], the peak at 1338 cm^{-1} corresponds to Ti-alkoxi bond [12] and the peak at 1604 cm^{-1} attributes to residue water [12,13]. The wide absorption peak centred at 3266 cm^{-1} designates to the hydroxyl group and bonded water. All absorption bands that found in as-prepared sample became disappeared after laser deposition of titania coatings which indicate the conversion of titania coatings into a new forms of titanium oxide. However, some weak absorption peaks observed at low wavenumber around 403 cm^{-1} that possibly come from the oxidation of the AISI316 substrates under the influence of laser energy.

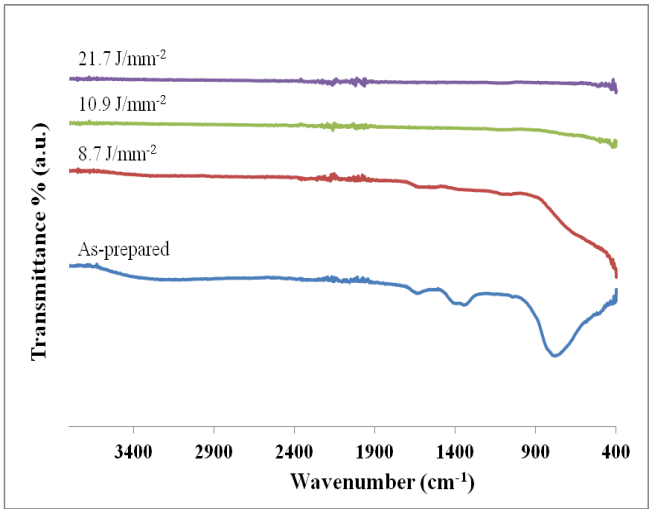

Figure 2. ATR-FTIR spectra of as-prepared and laser-deposited sol-gel titania coatings at various energies.

B. X-Ray Diffraction Analysis

XRD diffraction was employed to investigate the change of crystalline structure and phase composition of the laser-deposited titanium oxide coatings from titania sol. Fig. 3 shows the XRD diffraction patterns of typical titania samples. As shown in Fig. 3, the as-prepared sample (as reference) exhibits an amorphous structure, whilst the other samples indicate the formation of different crystalline structures of TiO_2 coatings after laser deposition. The intensity of both phases anatase and rutile-TiO_2 increased with the increase of laser energy. The diffraction peak at 25.22° can be referred to anatase phase, while the two peaks at 27.46° and 41.06° are corresponded to rutile [14-16]. Additional peaks of Ti_7O_{13} were detected at 28.6° and 29.46° assigned to sub stoichiometric titanium oxide [17], with the presence of $FeTiO_3$ at 32.57° that comes from the reaction between rutile-TiO_2 and hematite (α-Fe_2O_3) [14,18]. The peaks at 43.68° and 44.02° attribute to AISI316 substrates [19], whilst the presence of Fe_2O_3 peaks suggests the oxidation of the samples after laser irradiation [14]. The XRD results are consistent with the ATR-FTIR analysis, both confirming the change of composition and structure.

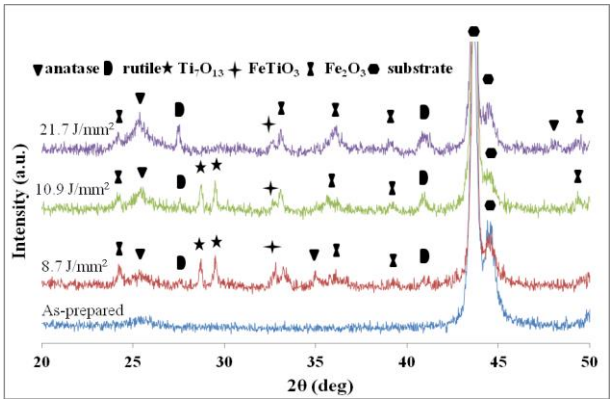

Figure 3. XRD patterns of as-prepared and laser-deposited sol-gel titania coatings at various energies

C. Surface Morphology

The characterisation of surface morphology of the laser-deposited titania coatings on the surface of AISI316 substrates at various energies was conducted by SEM. The SEM micrographs are illustrated in Fig. 4. The laser-deposited titania coatings show different surface morphologies after the deposition that depends on the laser energies delivered to the samples. The morphology of laser-deposited titania coating at 8.7 J/mm^2 shows a rough surface with texture like tree roots spread over the surface. Further increase of laser energy to 10.9 J/mm^2 lead to the deposition of titania coating with the development of some micro-cracks in the surface morphology. The deposited titania coating at the highest laser energy of 21.7 J/mm^2 exhibits a typical ceramic structure with large ceramic pieces.

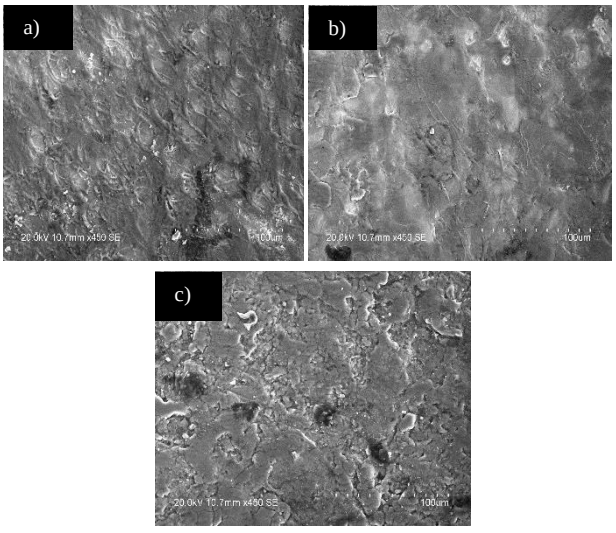

Figure 4. SEM micrographs of the deposited titanium coatings at various laser energies: (a) laser-deposited titania coatings at 8.7 J/mm^2, (b) laser-deposited titania coating at 10.9 J/mm^2 , and (c) laser-deposited titania coating at 21.7 J/mm^2 .

D. EDS Analysis

EDS technique was employed to study the change of elemental composition of laser-deposited titania coatings. The EDS results are summarised in Table II. It is clearly seen from Table1 that the titanium ratios are increased with the increase of the laser energy which indicates more titanium is formed. The element ration of titanium to oxygen for the as-prepared sample (as reference) is 1:19 which is far away from the elemental ratio of 1:2 in TiO_2. The elemental ratio of titanium to oxygen (T:O) for the laser-deposited titania coatings at 8.7 J/mm^2 and 10.9 J/mm^2 is 1:3 which is slightly away from the theoretical ratio of 1:2 in TiO_2. However, the deposited titania coating at the highest laser energy 21.7 J/mm^2 displays the optimal elemental ratio of 1:2 in TiO_2. The other elements of iron and chromium at different atomic percentages being picked up from the AISI316 substrates.

Table II. Elemental composition of laser-deposited titania coatings

Sample	**Atomic %**				
	O	**Ti**	**Fe**	**Cr**	**Ti:O**
As-prepared	54.13	2.79	29.23	8.17	1:19
8.7 J/mm^2	48.59	16.43	14.74	5.50	1:3
10.9 J/mm^2	63.31	20.19	2.49	11.36	1:3
21.7 J/mm^2	66.1	31.80	0.42	0.60	1:2

E. Mechanical Properties

Nanoindetation measurements were used to characterise the mechanical properties of the laser-deposited titania coatings on AISI316substrates. The loading –unloading profiles for the laser-deposit titania coatings at various energies are presented in Fig. 5. The laser-deposited titania coating at 8.7 J/mm^2 shows a maximum depth of circa 1050 nm at peak load. The laser-deposited titania coating at 10.9 J/mm^2 illustrates a maximum depth of approximately 750 nm at peak load. The deposited titania coating at laser energy of 21.7 J/mm^2 illustrates a maximum depth of around 270 nm at peak load. The decrease of indentation depth with the increase of laser energy indicates that the deposited titania coatings become more resistant to the nano-indentation indenter as a result of the crystalline nature of the deposited titania coatings.

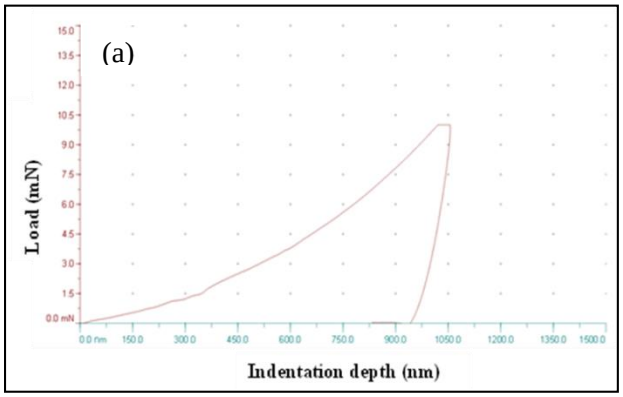

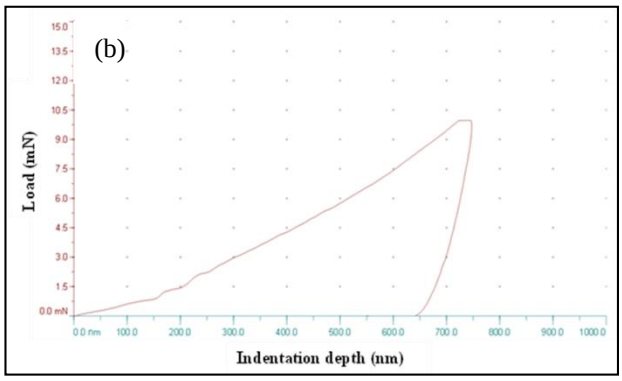

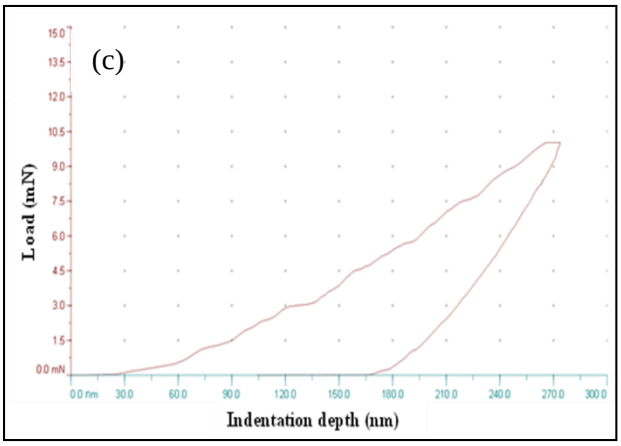

Figure 5. Typical nano-indentation test profile of load against indenting depth for laser-deposited titania coatings at : (a) 8.7 J/mm^2, (b) 10.9 J/mm^2 and 21.7 J/mm^2.

The values of hardness and Young's modulus of the laser-deposited titania coatings determined from the nano-indentation measurements are depicted in Table III. It is clearly seen that the hardness and Young's modulus of the deposited titania coatings are significantly improved with the increase of laser energy due to the phase-transition of anatase-TiO_2 into rutile-TiO_2 at the highest laser energy (as indicated clearly in XRD patterns).

Table III. Mechanical properties of laser-deposited titania coatings.

Sample	Laser energy	Hardness, *H* (GPa)	Young's modulus, *E* (GPa)
TiO_2-coating	8.7 J/mm^2	0.39	31.236
TiO_2-coating	10.9 J/mm^2	0.74	49.993
TiO_2-coating	21.7 J/mm^2	5.85	102.57

IV. CONCLUSION

The deposition of sol-gel titania coatings has been successfully achieved via fibre laser irradiation and sol-gel coating technology. The results confirmed the feasibility of using a combined laser/sol-gel technique to obtain crystalline titanium oxide coatings under wet condition. The ATR-FTIR analysis confirms the change of chemical composition of sol-gel titania coating after laser deposition. The XRD diffraction proves the crystallisation of the deposited titania coatings in both phases, anatase-TiO_2 and rutile-TiO_2 under the influence of laser irradiation. The SEM micrographs demonstrates that the laser irradiation leads to the deposition of sol-gel titania coating on the surface of AISI316 substrates. The EDS analysis proves that the laser-deposited titania coating reaches the optimal theoretical ratio of 1:2 in TiO_2. Nano-indentation results reveal that the hardness and Young's modulus of the deposited titania coatings show a significant improvement at the highest laser energy.

REFERENCES

[1] k. Khojier, H. Savaloni, H. Kangarloo, M. Ghoranneviss, M. Yari, appl. Surf. Sci. 254 (2008) 2528.

[2] E. Celik, A.Y. Yildiz, N.F. Ak Azem, M. Tanoglu, M. Toparli, O.F. Emrullahoglu, I. Ozdemir, Mater. Sci. Eng B129 (2006) 193.

[3] V. Yordanva, K. Starbova, W. Hintz, J. Tomas, U. Wendt. J. Optoelectron. Adv. Mater. 7 (2005) 2601.

[4] L. Castaneda, J.C. Alonso, A. Ortiz, E. Andrade, J.M Saniger, J.G. Banuelos, Mater. Chem. Phys. 77 (2002) 938.

[5] D. Siva Rama Krishna, Y. Sun, Surf. Coat. Techn. 198 (2005) 447.

[6] M.P. Moret, R. Zallen, D.P. Vijay, S.B. Desu, Thin. Solid. Films. 166 (2003) 176.

[7] Y.X. Leng, J.Y. Chen, P. Yang, H. Sun, N. Huang, Surf. Coat. Techn. 198 (2005) 447.

[8] Y.X. Leng, N. Huang, P. Yang, J.Y. Chen, H. Sun, J. Wang, G.J. Wan, Y. Leng, P.K. Chu, Thin. Solid. Films. 420-421 (2002) 408.

[9] Y.Z. Huang, D.J. Blackwood, Electrochim. Acta. 51 (2005) 1099.

[10] N. Sbai, J. Perriere, W. Seiler, E. Millon, Surf. Sci. 601 (2007) 5650.

[11] F.E. Ghodsi, F.Z. Tepehan, G.G. Tepehan, J. Phys. Chem. Solids 72 (2011) 763.

[12] M. Manso, S. Ogueta, P. Garcia, J.P. Rigueiro, C. Jimenez, J.M. Duart, M. Langlet, Biomaterials 23 (2002) 352.

[13] A.M. Seco, M.C. Goncalves, R.M. Almeida, Mater. Sci. Eng B76 (2000) 196.

[14] F. Liu, H. He, C. Zhang, Z. Feng, L. Zheng, Y. Xie, T. Hu, Appl. Catal. B: Environ 96 (2010) 413.

[15] F.H. Babaei, M. Keshmiri, M. Kakavand, T. Troczynski, Sens. Actuat. B 110 (2005) 30.

[16] K. Prasad, D.V. Pinjari, A.B. Pandit, S.T. Mhaske, Ultrasonics Sonochemistry. 17 (2010) 411.

[17] R. Tomaszek, L. Pawlowski, J. Zdanowski, J Grimblot, J. Laureyns, Surf. Coat. Techn. 185 (2004) 140-141.

[18] A. Khaleel, J. Colloids. Surface. 346 (2009) 132.

[19] C. Pflitsch, D. Viefhaus, U. Bergmann, B. Atakan, Thin Solid Films. 515 (2007) 3657.